Available online at www.sciencedirect.com
ScienceDirect
Journal of Magnetic Resonance 187 (2007) 216–224
JMR Journal of Magnetic Resonance
www.elsevier.com/locate/jmr

Applications of DNP-NMR for the measurement of heteronuclear T_1 relaxation times

Iain J. Day [a,b,*], John C. Mitchell [b], Martin J. Snowden [b], Adrian L. Davis [a]

[a] *Pfizer Global Research and Development, Sandwich Laboratories, Sandwich, Kent CT13 9NJ, UK*
[b] *Medway Sciences, University of Greenwich, Medway University Campus, Central Avenue, Chatham Maritime, Chatham, Kent ME4 4TB, UK*

Received 19 December 2006; revised 20 April 2007
Available online 6 May 2007

Abstract

Measurement of heteronuclear spin–lattice relaxation times is hampered by both low natural abundance and low detection sensitivity. Combined with typically long relaxation times, this results in extended acquisition times which often renders the experiment impractical. Recently a variant of dynamic nuclear polarisation has been demonstrated in which enhanced nuclear spin polarisation, generated in the cryo-solid state, is transferred to the liquid state for detection. Combining this approach with small flip angle pulse trains, similar to the FLASH-T_1 imaging sequence, allows the rapid determination of spin–lattice relaxation times. In this paper we explore this method and its application to the measurement of T_1 for both carbon-13 and nitrogen-15 at natural abundance. The effects of RF inhomogeneity and the influence of proton decoupling in the context of this experiment are also investigated.

Keywords: Dynamic nuclear polarisation; Spin–lattice relaxation; Heteronuclear

1. Introduction

Liquid-state dynamic nuclear polarisation (DNP) has recently been demonstrated as a method to significantly enhance the detection sensitivity of NMR spectroscopy [1–3]. This approach involves the generation of hyperpolarisation in the cryo-solid state, followed by the rapid transfer to solution state using a super heated dissolution solvent. The liquid sample is then transferred to a standard high resolution NMR spectrometer for detection [1,2]. Critical to the success of this technique is the ability to maintain the hyperpolarisation during the transfer process. Experience to date suggests that for simple systems a reasonable guide is provided in part by the solution-state high-field spin–lattice relaxation time, although this is not necessarily the complete picture [4]. Knowledge of an atom's spin–lattice relaxation time is also important when considering the correct choice of parameters for other more traditional experiments, especially the choice of recycle time in order to avoid any saturation effects or to maximise sensitivity for dilute solutions. DNP-NMR can provide a rapid method to obtain this parameter for dilute spins.

The direct measurement of carbon-13 and nitrogen-15 spin–lattice relaxation times is hampered by two major factors. The first is that these nuclei suffer from low sensitivity arising from both their low magnetogyric ratios and low natural abundance, 1.1% and 0.37%, respectively. Combined with this is the fact that these nuclei tend to have long relaxation times unless there are directly bonded protons. In general dipolar coupling to protons is the dominant relaxation mechanism. Relaxation arising from chemical shift anisotropy may become efficient at higher magnetic field strengths, especially for nuclei in aromatic environments of slowly tumbling molecules. Traditionally, carbon-13 and nitrogen-15 relaxation studies have been performed using concentrated samples in wide-diameter probes thereby increasing the detection sensitivity. These

* Corresponding author. Address: Medway Sciences, University of Greenwich, Medway University Campus, Central Avenue, Chatham Maritime, Chatham, Kent ME4 4TB, UK.
E-mail address: iain.day@pfizer.com (I.J. Day).

1090-7807/$ - see front matter © 2007 Elsevier Inc. All rights reserved.
doi:10.1016/j.jmr.2007.04.015

sensitivity issues and long relaxation times necessitate long data acquisition times, rendering $^{13}C/^{15}N$ relaxation time measurements at natural abundance a far from routine practice.

A variety of inverse-detection heteronuclear relaxation methods have been developed and widely adopted for the use in protein dynamics studies, most notably ^{15}N and ^{13}C relaxation data of the N^H, CO and C^α positions of the peptide backbone. These techniques are facilitated by uniform labelling of the carbon and nitrogen sites within the protein. In these labelled systems the sites of interest can easily be targeted by INEPT-type sequences using either the H^N or H^α proton to improve sensitivity. The simplest of these methods is a slight modification of the HSQC experiment in which a variable relaxation delay is following the t_1 evolution time [5]. The volumes of the HSQC peaks are monitored as a function of this relaxation delay. In small heteroaromatic molecules, for example those commonly found in pharmaceutical compounds, these methods are not so readily applicable. The prevalence of quaternary centres in these molecules tends to limit the number of atoms that can be accessed for study.

Traditionally, spin lattice relaxation times are measured using the inversion-recovery sequence [6]. This simple two-pulse scheme consists of an inversion pulse, either applied in a broadband manner to the whole spectrum, or as a band selective pulse to invert a particular resonance or multiplet of interest. Following this is an incremented delay during which the previously inverted magnetisation is allowed relax. A 90° read pulse is then applied to measure the recovered z-magnetisation as a function of this incremental delay. In order to ensure accurate quantification of the relaxation time it is necessary to ensure that there is complete return to thermal equilibrium between data points, hence typical recycle times for the inversion-recovery experiment are of the order of $5 \times T_1$. For carbon-13 and nitrogen-15 this can lead to recycle times of several minutes.

Matters can be improved by the use of the progressive-saturation experiment in which the inversion pulse is replaced by a series of randomly spaced and phased pulses with the aim of destroying all the z-magnetisation between data points. The remainder of the sequence is as for the inversion-recovery sequence. This technique does not require the use of long recycle times, however, is often considered less accurate as a smaller portion of the recovery profile is monitored and it is often difficult to reliably saturate the spectrum over the wide spectral widths associated with heteronuclear NMR.

Providing sufficient sensitivity is available there are a number of "fast" methods available for the acquisition of T_1 relaxation time data. These range from spatial encoding of the longitudinal magnetisation using field gradients enabling the complete relaxation profile to be obtained in a single acquisition [7], to experiments utilising trains of small flip angle pulses [8–11]. Both of these approaches have been widely adopted by the MRI community where total experiment duration is a critical design factor. The drawback of these methods, however, is that they require high signal to noise and offer no benefit when signal averaging is necessary. Hence these methods have only been routinely applied to abundant spins such as protons.

Recently it has been demonstrated that hyperpolarised nuclear spins can be generated in the cryo-solid state and successfully transferred to the liquid state, for detection in a standard high-resolution spectrometer [1]. This hyperpolarisation is generated using dynamic nuclear polarisation (DNP) in which a frozen solution of the compound of interest is irradiated with microwaves in the presence of a stable free radical. At cryogenic temperatures, there is significant electron spin polarisation present. The application of a microwave field at approximately the difference in electron and nuclear Larmor frequencies results in this polarisation being transferred to the nuclear spins [12,13]. Detection of this nuclear hyperpolarisation the liquid state is achieved by the use of a novel sample dissolution and transfer process [1–3]. This technique is somewhat similar to the solid-state DNP experiments performed by Griffin and co-workers [14–17], some of which employ an infrared laser to regenerate the solution state [18].

The presence of this hyperpolarisation enables many experiments to become feasible due to the increased signal to noise available. In this paper we demonstrate the application of the single-scan FT (SSFT) method proposed by Kaptein et al. for use in the rapid determination of heteronuclear spin–lattice relaxation times [11]. This method shares its approach with the Fast Low Angle SHot (FLASH) experiments developed by Haase and co-workers for use in MRI studies [8–10].

The combination of DNP-generated hyperpolarisation using the Ardenkjaer–Larsen method [1] and the SSFT/FLASH method allows heteronuclear spin–lattice relaxation times to be determined on a time scale which is governed only by the time required to generate the nuclear polarisation.

2. Methods

2.1. NMR data acquisition

All NMR data were acquired using a 2-channel Varian Unity INOVA 500 spectrometer with a 5 mm X{^{1}H} switchable probe for observation of ^{13}C or ^{15}N equipped with a z-gradient.

2.2. Inversion recovery

Inversion-recovery experiments were performed using 5 mg of uniformly carbon-13 labelled sodium acetate dissolved in 1 mL of methanol-d_4. For comparison with the DNP-enhanced measurement, 375 μM of stable trityl radical was added to a second sample. This was the same concentration as present after dissolution in the hyperpolarised experiment. In either case, the samples were not degassed

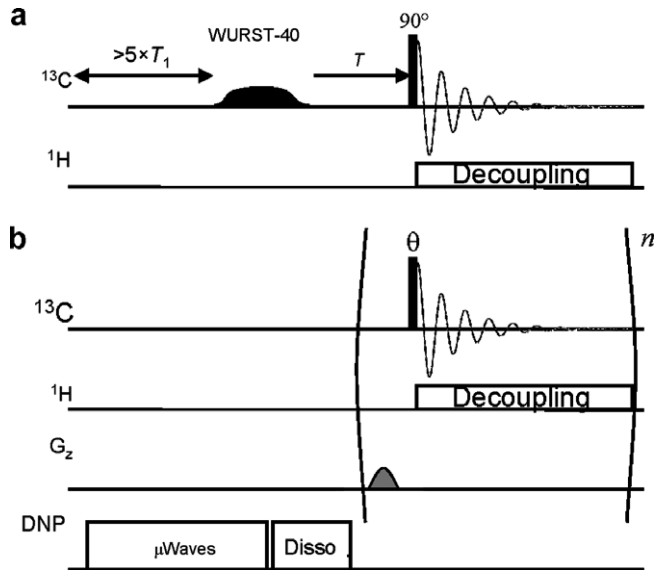

Fig. 1. (a) Pulse sequence used for the inversion recovery experiments. The initial inversion pulse was an adiabatic pulse with the WURST-40 waveform. Proton decoupling was implemented either using WALTZ-16 modulation, or with $2n$ WURST-40 adiabatic pulses applied with the M4T5 supercycle. (b) Shows the pulse sequence timing diagram used for the DNP-T_1 measurements. θ represents a small flip angle pulse, usually 25°. Proton decoupling was applied using the same methods as for the inversion recovery pulse sequence.

prior to use. The classic two-pulse sequence was used with only minor modifications. The initial inversion pulse was a 1.5 ms adiabatic broadband inversion pulse using the WURST-40 waveform. The schematic timing diagram is shown in Fig. 1a. Proton decoupling was implemented using the WALTZ-16 modulation scheme [19] and if applied, used either only during acquisition, or for the duration of the experiment. Recycle times for these experiments were greater than 600 s to ensure complete return to thermal equilibrium between data points. Data sets were analysed using a two parameter single exponential fit to the experimental traces using the Levenburg–Marquardt algorithm as implemented in the SciPy modules of the Python programming language [20].

2.3. Dynamic nuclear polarisation

Dynamic nuclear polarisation experiments were performed using a *HyperSense* DNP polariser (Oxford Instruments Molecular Biotools Ltd, Eynsham, UK). The samples were as follows: 10 mg of acetaminophen or 25 mg of nicotinamide, both at natural abundance, were dissolved in 50 μL of dimethyl sulphoxide and 50 μL of methanol containing 15 mM of a trityl-based stable free radical [21]. The sample was then placed in the *HyperSense* instrument and frozen in liquid helium at 1.4 K in a static magnetic field of 3.35 T. W-band microwave irradiation was then applied at approximately the difference in electron and nuclear Larmor frequencies (~94.085 GHz for ^{13}C or ~94.098 GHz for ^{15}N). The exact microwave frequency for carbon-13 was determined by sweeping the microwave frequency to find the maximum solid-state polarisation signal. For nitrogen-15 the microwave frequency was calibrated from the carbon-13 frequency determined above with data from an Oxford Instruments research polariser (D. Blazina and S. Reynolds, personal communication). Following a pre-determined polarisation time, typically 3 h, the sample was dissolved using 4 mL of methanol heated to a temperature of ~410 K at a pressure of 9 bar, and transferred to the high resolution NMR spectrometer along a PTFE hose into the waiting NMR tube using helium gas. Data acquisition was triggered by a TTL pulse from the *HyperSense* instrument to the acquisition controller card of the NMR spectrometer. The typical solution transfer time was 3 s. The final radical concentration in the methanol solution was 375 μM. SSFT/FLASH relaxation data were collected with the pulse sequence shown in Fig. 1b. Spectra were acquired using a train of small flip angle pulses θ, usually 25°, spaced one second apart with data acquisition during the first 500 ms of this period. The spectra were obtained over a spectral width of 31 kHz. Each repetition of the sequence includes the application of a pulsed field gradient to dephase any remaining transverse magnetisation at the end of the acquisition time and hence remove any T_2-interference artefacts [6]. Proton decoupling was performed either using the WALTZ-16 modulation scheme, during acquisition or for the duration of the experiment, or using WURST-40 adiabatic pulses, with the M4T5 modulation scheme, adjusting the acquisition time such that it was spanned by $2n$ pulses [22].

2.4. Magnetisation dynamics

The magnetisation dynamics under this pulse sequence have been derived by Kaptein et al. [11] following initial work by Look and Locker [23]. The analysis also follows similarly for the FLASH-T_1 imaging experiment [8–10]. The salient details are repeated here for clarity. Consider the initial magnetisation produced by the DNP experiment M_{DNP}. Following the first θ pulse the remaining magnetisation along the z-axis is given by:

$$M_z(0+) = M_{\mathrm{DNP}} \cos\theta \tag{1}$$

Assuming that the longitudinal relaxation during the subsequent free induction decay can be described by a single exponential with time constant T_1, then the z-magnetisation present prior to the time of the next θ pulse is:

$$M_z(T) = M_{\mathrm{DNP}} \cos\theta \exp(-T/T_1) + M_0[1 - \exp(-T/T_1)] \tag{2}$$

where T is the time between RF pulses, usually equal to the acquisition time. The first term in this expression corresponds to the decay of the hyperpolarised magnetisation and the latter term to the recovery of the magnetisation excited by the RF pulse to its thermal value. As a simplification

let $\alpha = \cos\theta$ and $\beta = \exp(-T/T_1)$. Continuing Eq. (2) following the second pulse and acquisition gives:

$$M_z(2T) = M_{DNP}\alpha^2\beta^2 + M_0(1-\beta)(1+\alpha\beta) \quad (3)$$

Therefore, generalising this to n data points results in the following equation:

$$M_z(nT) = M_{DNP}\alpha^n\beta^n + M_0(1-\beta)\sum_{j=0}^{n-1}(\alpha\beta)^j \quad (4)$$

The summation term in Eq. (4) describes a converging geometric series. Since α and β are both less than unity, this expression can be simplified to:

$$M_z(nT) = M_{DNP}\alpha^n\beta^n + M_0(1-\beta)\frac{1-\alpha^n\beta^n}{1-\alpha\beta} \quad (5)$$

The transverse magnetisation after each pulse, which is proportional to the observed signal, is:

$$M_{x/y}(nT) = M_z(nT)\sin\theta \quad (6)$$

A gradient pulse is applied at the end of the acquisition period to ensure that any remaining transverse magnetisation does not interfere with subsequent data points.

2.5. Effects of B_1 inhomogeneity

Inhomogeneities of the B_1 RF field result in an average under-rotation of the magnetisation vector by the RF pulse [6]. In the context of this analysis, B_1 inhomogeneity effects will be manifest in T_1 parameters which deviate from their true value. The extent of this B_1 inhomogeneity can be measured using a standard nutation experiment and analysing the data obtained in terms of an exponentially-damped sinusoidal function of pulse length. The following empirical expression gives the magnitude of the observed magnetisation as a function of the RF pulse length τ_p:

$$S(\theta) = A\sin(\gamma B_1\tau_p)\exp(-f\gamma B_1\tau_p) \quad (7)$$

where A is an scaling term and f is a parameter characterising the RF inhomogeneity. The B_1 homogeneity of a probe is often quoted in terms of the ratio of the signal intensity for a 450° rotation compared to a 90° rotation. The inhomogeneity parameter f is linked to this ratio by $S(450/90) = \exp(-2\pi f)\times 100\%$.

To determine the B_1 RF inhomogeneity of the probe used in this study a nutation experiment was carried out placing the methyl group of ^{13}C-labelled sodium acetate, or the amide nitrogen of ^{15}N-labelled benzamide on resonance, and varying the ^{13}C or ^{15}N RF pulse width as appropriate (data not shown). Fitting Eq. (7) to the data allowed the RF field strength and inhomogeneity parameters to be extracted. These values are presented in Table 1 and are typical for probes of this configuration.

Table 1
RF field strength and inhomogeneity parameters for the inner coil of the X{^{1}H} probe

Nucleus	$\gamma B_1/2\pi$ (kHz)	f	$S(450/90)$
^{13}C[a]	34.16 ± 0.01	0.0159 ± 0.0008	90.50%
^{15}N[b]	16.98 ± 0.01	0.0283 ± 0.0012	83.72%

[a] Methyl carbon of ^{13}C-labelled sodium acetate.
[b] Amide nitrogen of ^{15}N-labelled benzamide.

Combining the influence of B_1 inhomogeneity with the magnetisation dynamics during the SSFT/FLASH experiment gives the following expression which was used in the analysis described in this paper:

$$M_{x/y}(nT) = \left\{M_{DNP}\alpha^n\beta^n\exp(-nf\theta) + M_0(1-\beta)\frac{1-\alpha^n\beta^n\exp(-nf\theta)}{1-\alpha\beta\exp(-f\theta)}\right\} \times \sin\theta\exp(-f\theta) \quad (8)$$

The dynamics of the z-magnetisation described by this equation are demonstrated in Fig. 2 for a series of flip angles. It can be seen that smaller flip angles give a smaller rate of signal decay, albeit at the expense of overall sensitivity.

2.6. Obtaining T_1 from SSFT/FLASH data

As outlined above, the z-magnetisation dynamics occurring during the pulse sequence shown in Fig. 1b can be described by Eq. (8), including the correction for the effects of B_1 RF inhomogeneity. Each resonance included in the analysis was allowed variable T_1 and M_{DNP} values, with all resonances sharing a global value of the thermal polarisation M_0. Eq. (8) was fitted to the experimental traces using the Levenburg–Marquardt algorithm as implemented in the SciPy modules of the Python programming language [20]. For the experiments presented in this paper, the flip angle was set to 25° and the repetition time T was 1 s.

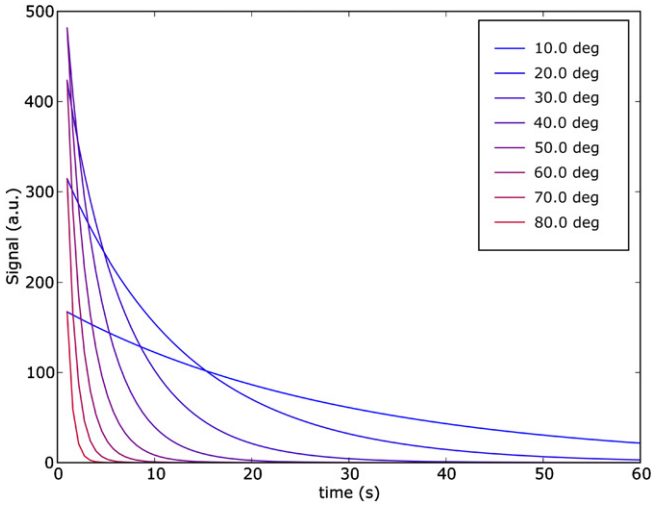

Fig. 2. z-magnetisation dynamics as a function of various flip angles θ for the pulse sequence shown in Fig. 1b. This figure was calculated for a recycle time of 1 s using a T_1 of 45 s with a DNP-induced signal enhancement of 1000-fold. The B_1 inhomogeneity parameter was set to $f = 0.0159$ as determined from the ^{13}C nutation experiment described in the text.

2.7. Parameter error estimation

Standard deviations in the fitted parameters were estimated using Monte Carlo methods, typically with 1000 realisations. In brief, synthetic data sets were generated using the parameters obtained from either the two-parameter fit in the case of the inversion-recovery data, or from fitting Eq. (8) to the SSFT/FLASH data. To these synthetic data, Gaussian noise with zero mean and standard deviation equal to that of the original fitted residuals was added. The synthetic data were then re-analysed and a distribution of fitted parameters obtained. From this, the standard deviations in the fitted parameters were estimated. No change in the estimated standard deviations was found by increasing the number of realisations.

3. Results and discussion

3.1. Comparison with inversion recovery

The reliability of the SSFT/FLASH method for determining spin–lattice relaxation times was tested by comparison with the ^{13}C relaxation times measured using the standard inversion-recovery approach. These data are presented in Table 2. In this case, the SSFT/FLASH measurements were performed using the thermal polarisation available on uniformly labelled carbon-13 sodium acetate. Clearly in the absence of any proton decoupling the two methods yield similar results, for example the inversion recovery and SSFT/FLASH measurements yield T_1 values of 37.95 ± 0.28 s and 38.15 ± 0.38 s for the carboxyl group, respectively. The situation is similar for the methyl group. When DNP is used to enhance the sensitivity of the SSFT/FLASH measurement the results are very similar, as evidenced by the last row in Table 3. Therefore, in the absence of decoupling the SSFT/FLASH method gives good agreement with the traditional approach of inversion recovery.

3.2. Effects of decoupling

Traditional carbon-13 NMR spectroscopy exploits the fact that the carbon signals can be enhanced by the generation of an NOE from attached protons. This is usually performed by gating the decoupler channel on during the recycle periods of the experiment as well as during the acquisition. For the DNP experiment, the generation of the NOE is not necessary for sensitivity, as decoupling is used merely to remove splitting arising from J-coupling and reduce the line width arising from unresolved couplings. In the context of the SSFT/FLASH approach presented here for the measurement of T_1, the use of decoupling presents a complication, even during the acquisition period, which may shorten the apparent relaxation time due to magnetisation transfer from the attached protons, hence leading to a measured T_1 value which is smaller than the true relaxation time. This effect can be clearly observed for both the inversion recovery derived data, when the decoupler is used throughout the experiment, and for the SSFT/FLASH method, the values of T_1 obtained are shown in Table 2. Limited influence is observed for inversion recovery when the decoupler duty cycle is low, i.e. when decoupling is only applied during acquisition. The generation of the NOE during the SSFT/FLASH approach in fact renders the T_1 analysis impossible for the directly protonated methyl group of sodium acetate and significantly shortens the measured relaxation time for the quaternary carboxyl carbon. Recently Piotto and co-workers developed a modification of the DEFT experiment which presents decoupled data which is devoid of NOE interference [22]. This was achieved by the use of an even number of adiabatic decoupling pulses during acquisition of the FID. The idea behind this is to leave reliably the proton magnetisation along the $+z$ axis at the conclusion of the acquisition period. As this magnetisation is left in an equilibrium position the potential for the growth of an NOE is severely reduced. Tenailleau and Akoka have also discussed recently the use of adiabatic decoupling schemes for accurate determination of ^{13}C intensity measurements [24]. Table 2 shows relaxation times obtained using the SSFT/FLASH measurement performed with WURST-40 decoupling, adjusting the acquisition time to encompass $2m$ repetitions of the T5M4 supercycle i.e. $40m$ decoupling pulses.

In the case of the quaternary carboxyl group the use of the adiabatic decoupling scheme almost completely removes the influence of the decoupler-induced NOE on the measured spin–lattice relaxation time. The effects are not quite so pronounced, however, for the methyl group.

Table 2
T_1 values obtained for the carboxyl and methyl carbons of labelled sodium acetate in the absence of radical

Pulse sequence	Decoupling scheme	Carboxyl (s)	Methyl (s)
Inversion recovery	No decoupling	37.95 ± 0.28	11.89 ± 0.09
	WALTZ (acq. only)	37.27 ± 0.13	10.82 ± 0.06
	WALTZ (continuous)	30.08 ± 0.20	10.18 ± 0.03
	WURST (acq. only)	n/r	n/r
SSFT/FLASH T_1	No decoupling	38.15 ± 0.38	13.20 ± 0.36
	WALTZ (acq. only)	23.51 ± 0.24	n/d
	WALTZ (continuous)	19.05 ± 0.24	n/d
	WURST (acq. only)	34.77 ± 0.45	3.42 ± 0.14

n/r, not recorded; n/d, not determined.

Table 3
T_1 values obtained for the carboxyl and methyl carbons of labelled sodium acetate in the presence of 375 μM radical

Pulse sequence	Decoupling scheme	Carboxyl (s)	Methyl (s)
Inversion recovery	No decoupling	39.16 ± 0.31	11.87 ± 0.05
	WALTZ (acq. only)	38.40 ± 0.15	10.68 ± 0.05
	WALTZ (continuous)	31.91 ± 0.42	10.23 ± 0.06
	WURST (acq. only)	n/r	n/r
SSFT/FLASH T_1	No decoupling	37.93 ± 0.31	13.40 ± 0.37
	WALTZ (acq. only)	23.51 ± 0.23	n/d
	WALTZ (continuous)	19.04 ± 0.22	n/d
	WURST (acq. only)	38.06 ± 0.53	3.87 ± 0.14
SSFT/FLASH T_1 with DNP	No decoupling	37.18 ± 1.62	11.62 ± 0.32

n/r, not recorded; n/d, not determined.

The relaxation time obtained for this carbon are only 15% of the true T_1 value. This is due to a number of factors, principally that the proton magnetisation will be in a non-equilibrium state due to decoupling pulses hence there is still scope for the generation of a $^{13}C\{^1H\}$ NOE. Cross relaxation, which has an r^{-6} distance dependence in simple cases, will necessarily be more pronounced for the methyl group compared with the carboxyl carbon. Secondly there is also the cumulative influence of minor imperfections in the decoupling scheme and phase cycle. Tenailleau and Akoka suggest that a longer supercycle of the decoupling pulses provides more accurate decoupling [24], however, this would impose impractical limits on the acquisition time as their suggested M4P5-M4P9-M4P5′-M4P9′ supercycle would require multiples of 224 decoupler pulses [24]. Therefore the decision to use decoupling and the manner in which it is applied depends on the nature of the parameter wished to be obtained—whether this is a phenomenological T_1 to determine repetition rate and sensitivity for further experiments, or a relaxation time suitable for molecular dynamics studies and determination of correlation times.

3.3. Effect of radical presence

In order to determine the influence of the radical present post-dissolution on the rate of spin–lattice relaxation, both inversion recovery and SSFT/FLASH relaxation profiles were measured in the presence and absence of the radical. Table 3 shows the relaxation times obtained for the same set of experiments as shown in Table 2. The differences between the values obtained by these methods are not significant to within the error inherent in the experiment. Significantly larger quantities of radical would be required to produce a noticeable effect [25]. For example, approximately 50 mM $Cr(acac)_3$ is required to produce a contribution to the relaxation rate of $\approx 10\ s^{-1}$ of carbon atoms within a molecule [25]. Any effect is most pronounced where the paramagnetic contribution to relaxation is the dominant one, e.g. for non-protonated carbon atoms. A small contribution from the presence of the radical to the proton spin–lattice relaxation rate of the methyl group in sodium acetate was measured to be $3.5 \times 10^{-3}\ s^{-1}$ at 375 μM radical. Any effect on the carbon nuclei must be significantly smaller, as already stated. Therefore, at the radical concentration required by the DNP experiment there is no detectable contribution to the carbon relaxation.

3.4. Natural abundance ^{13}C T_1 measurements with HyperSense DNP-NMR

The approach described in this paper is not limited to isotopically labelled species. The use of DNP to generate nuclear hyperpolarisation allows this method to be used to determine spin–lattice relaxation times of heteronuclei at natural abundance. This is demonstrated using the compound acetaminophen, which contains a number of different carbon sites of interest as shown in Fig. 3a. Three carbons have no attached protons, and would be expected to have longer relaxation times than either the tertiary aromatic carbons or the methyl carbon of the *N*-acetyl group.

The SSFT/FLASH experiment with DNP-generated hyperpolarisation was performed using a polarisation time of approximately three hours. To limit the influence of the proton decoupling on the measured values of T_1, adiabatic decoupling using WURST-40 pulses was applied during the acquisition period, i.e. a duty cycle of 50%. Fig. 3b shows the aromatic region in a stacked-plot representation of the series of spectra obtained, spaced at one second intervals. The five resonances in this region all clearly show an exponential-like decay as would be expected from this theory outlined in the methods section. The decay of the magnetisation was then analysed in terms of Eq. (8), the experimental data and the least-squares fit are shown in Fig. 3c. The spin–lattice relaxation times obtained for acetaminophen, presented in Table 4, are all in the range to be expected for a small molecule in the fast tumbling regime [26].

From the parameters extracted using Eq. (8) it may be thought that the magnitude of DNP enhancement could be calculated. However, in the case of measurements performed at natural abundance when the thermal spectrum is not obtainable in a single scan, the M_0 parameter in

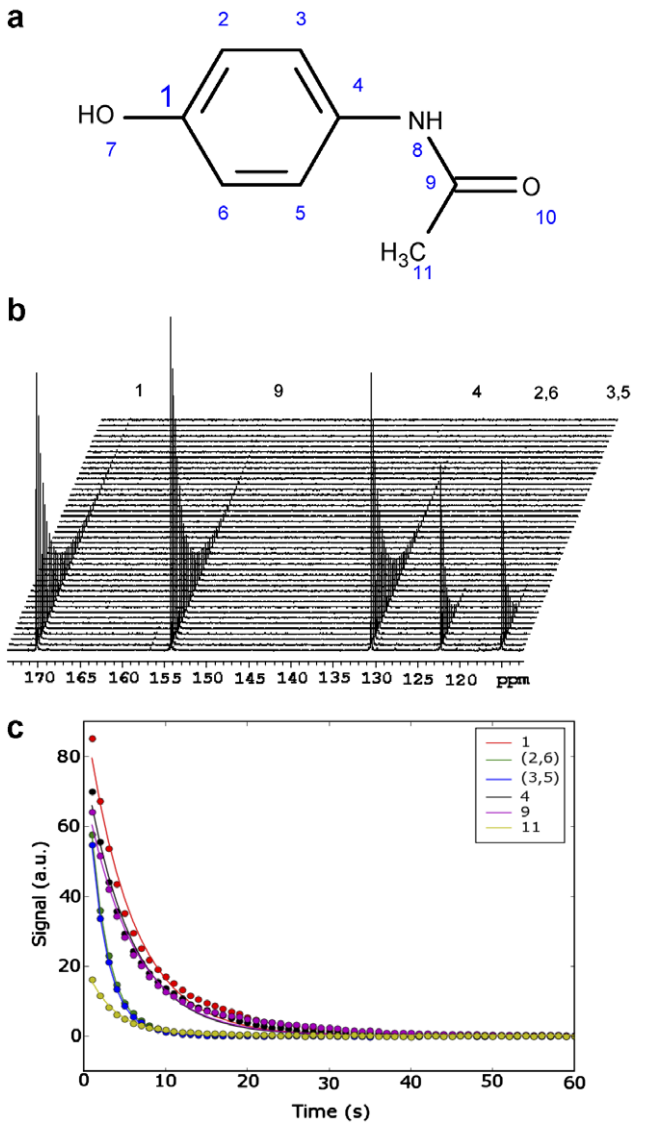

Fig. 3. DNP-generated SSFT/FLASH T_1 measurement for acetaminophen at natural abundance. (a) Shows the structure and numbering scheme for acetaminophen (*N*-(4-hydroxyphenyl)acetamide). (b) Shows the aromatic region of the ^{13}C NMR spectra obtained using the pulse sequence shown in Fig. 1b. (c) Shows the analysis of the signal intensities in terms of the *z*-magnetisation dynamics described in Eq. (8).

Table 4
^{13}C spin–lattice relaxation times (in seconds) for acetaminophen

Atom	T_1 (s)	M_{DNP}[a]
1	30.11 ± 2.41	186.8 ± 2.1
2,6	3.20 ± 0.14	178.0 ± 5.0
3,5	3.04 ± 0.14	171.9 ± 4.8
4	26.77 ± 2.40	155.6 ± 2.2
9	37.34 ± 4.85	141.1 ± 2.1
11	6.86 ± 1.46	40.8 ± 3.2

[a] $M_0 = 0.86 \pm 0.24$.

general cannot be accurately extracted from the fitting process. In fact, setting $M_0 = 0$ during the fitting procedure, i.e. neglecting the second term in Eq. (6), results in an insignificant change in the extracted parameters. If one is able to measure the thermal polarisation in a single scan e.g. by the use of isotopically labelled samples, then an accurate value of M_0 would be obtained, and hence the DNP-generated enhancement can be calculated. This enhancement can also be determined from an independent measure of the thermal polarisation.

In order to estimate the overall sensitivity gain achieved using DNP consider that using labelled sodium acetate the inversion recovery experiment required a total experiment time of 8 h 45 min, with one scan per data point. To achieve the same level of sensitivity for an unlabelled sample would take approximately 98.9^2 times longer. The DNP-based approach achieves similar levels of sensitivity on an unlabelled sample with only a few hours polarisation time, the enhancement offered therefore is on the order of 10,000-fold.

3.5. Natural abundance ^{15}N T_1 measurements with HyperSense DNP-NMR

While observation of carbon-13 at natural abundance is a routine experiment, direct observation of nitrogen-15 is generally not popular due to the lower natural abundance (0.37%) and the lower magnetogyric ratio. DNP can be used to mitigate this sensitivity loss and in combination with the SSFT/FLASH method can be used to determine ^{15}N T_1 relaxation times in the same manner as for carbon-13.

Nicotinamide was chosen as a representative compound (Fig. 4a), as it contains two distinct nitrogen sites: an aromatic pyridine-like nitrogen and a protonated amide nitrogen. The SSFT/FLASH spectra generated following polarisation for five hours are shown in Fig. 4b. As found for acetaminophen, the nicotinamide spectra show the expected trends. Fitting these traces to Eq. (8) gives the results plotted in Fig. 4c with the T_1 values extracted presented in Table 5. These values are within the range expected for the different nitrogen types present within nicotinamide [27].

4. Conclusions

In this paper we have demonstrated a new method which allows spin–lattice relaxation times of heteronuclei at natural abundance to be obtained with reasonable accuracy. This approach utilises the sensitivity advantage conferred by the use of dynamic nuclear polarisation and combines this with a train of small flip angle pulses. Together this allows the spin–lattice relaxation time to be determined without the need to use long recycle times on the order of $5 \times T_1$. The time scale of the experiment is limited purely by the time required to generate the hyperpolarisation, typically 2–3 h. For nuclei with low natural abundance, such as carbon-13 or nitrogen-15, this represents a total reduction in experimental time on the order of 10,000. Using this hyperpolarisation allows heteronuclear T_1 values to be estimated without isotopic

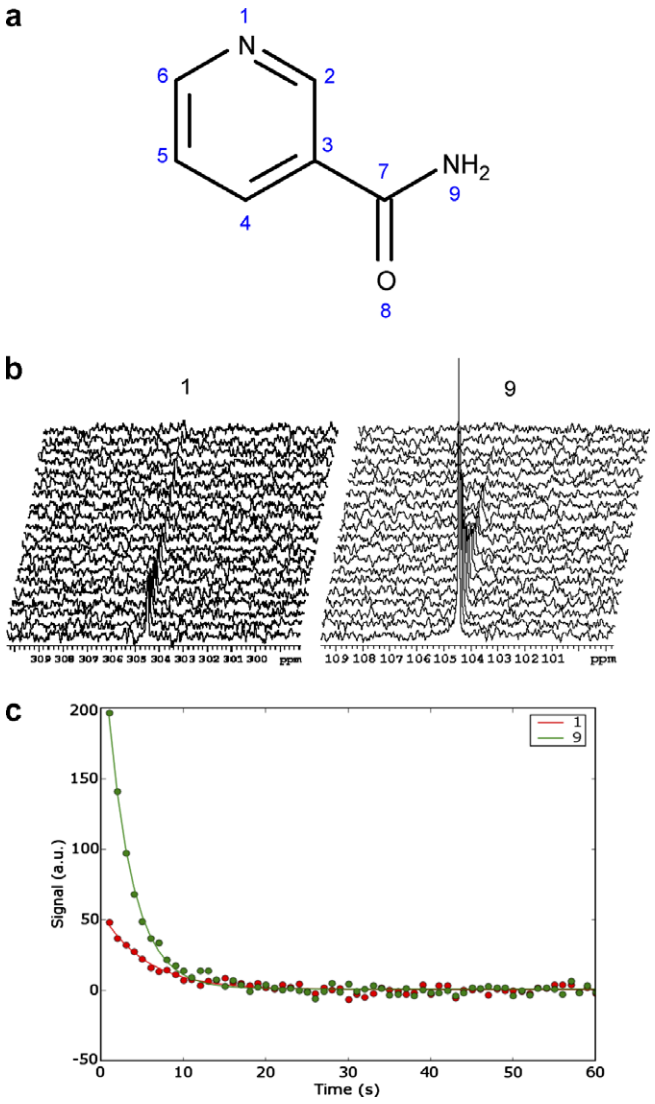

Fig. 4. DNP-generated SSFT/FLASH T_1 measurement for nicotinamide at natural abundance. (a) Shows the structure and numbering scheme for nicotinamide (pyridine-3-carboxamide). (b) Shows the aromatic region of the ^{15}N NMR spectra obtained using the pulse sequence shown in Fig. 1b. (c) Shows the analysis of the signal intensities in terms of the z-magnetisation dynamics described in Eq. (8).

Table 5
^{15}N spin–lattice relaxation times (in seconds) for nicotinamide

Atom	T_1 (s)	M_{DNP}[a]
1	16.69 ± 4.77	114.0 ± 6.38
9	4.91 ± 0.18	554.8 ± 9.76

[a] $M_0 = 2.18 \pm 1.17$.

enrichment. This benefit is especially apparent for nuclei with low natural abundance such as nitrogen-15. The approach described in this paper should be readily applicable to the determination of spin–lattice relaxation times of any low-frequency spin-1/2 nucleus. Although proton decoupling is convenient, it has been shown to be a complicating factor and recommendations to minimise the impact on T_1 estimation have been made.

The spin–lattice relaxation time appears to be an important parameter for determining the success of liquid state DNP generated using the Ardenkjaer–Larsen method. In future we will use these experiments to explore systematically the applicability of the DNP experiment for enhancing carbon-13 and nitrogen-15 detection sensitivity, and determine the contributions from molecular structure, solution T_1 or other effects. This methodology may also be adapted to combine T_1 and frequency modulation, thereby allowing the acquisition of two-dimensional correlation experiments [28].

Acknowledgments

We are grateful to Dr Andy Sowerby and Andrew Illsley of Oxford Instruments Molecular Biotools Ltd. for enabling this collaborative project. We thank Drs Damir Blazina, Steven Reynolds, Profs. Geoff Hawkes and Ulrich Günther for stimulating discussions, and Prof. P. J. Hore for insightful comments during the preparation of the manuscript.

References

[1] J.H. Ardenkjaer-Larsen, B. Fridlund, A. Gram, G. Hansson, G. Hansson, M.H. Lerche, R. Servin, M. Thaning, K. Golman, Increase in signal-to-noise ratio of >10,000 times in liquid-state NMR, Proc. Natl. Acad. Sci. USA 100 (2003) 10158–10163.
[2] J. Wolber, F. Ellner, B. Fridlund, A. Gram, H. Johannesson, G. Hansson, L.H. Hansson, M.H. Lerche, S. Mansson, R. Servin, M. Thaning, K. Golman, J.H. Ardenkjaer-Larsen, Generating highly polarized spins in solution using dynamic nuclear polarization, Nuc. Inst. Methods Phys. Res. A 526 (2004) 173–181.
[3] K. Golman, J.H. Ardenkjaer-Larsen, J.S. Petersson, S. Mansson, I. Leunbach, Molecular imaging with endogenous substances, Proc. Natl. Acad. Sci. USA 100 (2003) 10435–10439.
[4] K. Miesel, K.L. Ivanov, A.V. Yurkovskaya, H.-M. Vieth, Coherence transfer during field-cycling NMR experiments, Chem. Phys. Lett. 425 (2006) 71–76.
[5] L.E. Kay, D.A. Torchia, A. Bax, Backbone dynamics of proteins as studied by ^{15}N inverse detected heteronuclear NMR spectroscopy: application to staphylococcal nuclease, Biochemistry 28 (1989) 8972–8979.
[6] R.R. Ernst, G. Bodenhausen, A. Wokaun, Principles of Nuclear Magnetic Resonance in One and Two Dimensions, Oxford University Press, Oxford, 1990.
[7] N.M. Loening, M.J. Thrippleton, J. Keeler, R.G. Griffin, Single-scan longitudinal relaxation measurements in high-resolution NMR spectroscopy, J. Magn. Reson. 164 (2003) 321–328.
[8] A. Haase, Snapshot FLASH MRI. Applications to T1, T2 and chemical shift imaging, Magn. Reson. Med. 13 (1990) 77–89.
[9] R. Deichmann, A. Haase, Quantification of T1 values by SNAPSHOT-FLASH NMR imaging, J. Magn. Reson. 96 (1992) 608–612.
[10] R. Deichmann, D. Hahn, A. Haase, Fast T1 mapping on a whole-body scanner, Magn. Reson. Med. 42 (1999) 206–209.
[11] R. Kaptein, K. Dijkstra, C.E. Tarr, A single-scan Fourier transform method for measuring spin–lattice relaxation times, J. Magn. Reson. 24 (1976) 295–300.
[12] A. Abragam, Principles of Nuclear Magnetism, Oxford University Press, Oxford, 1961.
[13] A. Abragam, M. Goldman, Principles of dynamic nuclear polarisation, Rep. Prog. Phys. 41 (1978) 395–467.

[14] M. Rosay, V. Weis, K.E. Kreischer, R.J. Temkin, R.G. Griffin, Two-dimensional ^{13}C–^{13}C correlation spectroscopy with magic angle spinning and dynamic nuclear polarization, J. Am. Chem. Soc. 124 (2002) 3214–3215.

[15] M. Rosay, J.C. Lansing, K.C. Haddad, W.W. Bachovchin, J. Herzfeld, R.J. Temkin, R.G. Griffin, High-frequency dynamic nuclear polarization in MAS spectra of membrane and soluble proteins, J. Am. Chem. Soc. 125 (2003) 13626–13627.

[16] K.-N. Hu, H.-H. Yu, T.M. Swager, R.G. Griffin, Dynamic nuclear polarization with biradicals, J. Am. Chem. Soc. 126 (2004) 10844–10845.

[17] P.C.A. van der Wel, K.-n. Hu, J. Lewandowski, R.G. Griffin, Dynamic nuclear polarization of amyloidogenic peptide nanocrystals: GNNQQNY, a core segment of the yeast prion protein Sup35p, J. Am. Chem. Soc. 128 (2006) 10840–10846.

[18] C.-g. Joo, K.-n. Hu, J.A. Bryant, R.G. Griffin, In situ temperature jump high-frequency dynamic nuclear polarisation experiments: enhanced sensitivity in liquid-state NMR spectroscopy, J. Am. Chem. Soc. 128 (2006) 9428–9432.

[19] A.J. Shaka, J. Keeler, T. Frenkiel, R. Freeman, An improved sequence for broadband decoupling: WALTZ-16, J. Magn. Reson. 53 (1983) 335–338.

[20] E. Jones, T. Oliphant, P. Peterson, et al., SciPy: Open Source Scientific Tools for Python, 2001.

[21] D. Blazina, S. Reynolds, R. Slade, Application Note: Influence of Trityl Radical on the DNP Process, Oxford Instruments Molecular Biotools Ltd., 2006.

[22] M. Piotto, M. Bourdonneau, K. Elbayed, J.-m. Wieruszeksi, G. Lippens, New DEFT sequences for the acquisition of one-dimensional carbon NMR spectra of small unlabelled molecules, Magn. Reson. Chem. 44 (2006) 943–947.

[23] D.C. Look, D.R. Locker, Time saving in measurement of NMR and EPR relaxation times, Rev. Sci. Instru. 41 (1970) 250–251.

[24] E. Tenailleau, S. Akoka, Adiabatic ^{1}H decoupling scheme for very accurate intensity measurements in ^{13}C NMR, J. Magn. Reson. 185 (2007) 50–58.

[25] F.W. Wehrli, T. Wirthlin, Interpretation of carbon-13 NMR spectra, Heyden and Son Ltd., London, 1976.

[26] G.C. Levy, R.L. Lichter, G.L. Nelson, Carbon-13 nuclear magnetic resonance spectroscopy, Wiley-Interscience, New York, 1980.

[27] G.C. Levy, R.L. Lichter, Nitrogen-15 nuclear magnetic resonance spectroscopy, Wiley-Interscience, New York, 1979.

[28] C.E. Lyon, J.A. Jones, C. Redfield, C.M. Dobson, P.J. Hore, Two-dimensional ^{15}N–^{1}H photo-CIDNP as a surface probe of native and partially structured proteins, J. Am. Chem. Soc. 121 (1999) 6506.